

SeqScreen: Accurate and Sensitive Functional Screening of Pathogenic Sequences via Ensemble Learning

Advait Balaji*¹, Bryce Kille*¹, Anthony D. Kappell², Gene D. Godbold³, Madeline Diep⁴, R. A. Leo Elworth¹, Zhiqin Qian¹, Dreycey Albin¹, Daniel J. Nasko⁵, Nidhi Shah⁵, Mihai Pop⁵, Santiago Segarra⁶, Krista L. Ternus^{#2}, and Todd J. Treangen^{#1}

¹ Department of Computer Science, Rice University, Houston, TX

² Signature Science, LLC, 8329 North Mopac Expressway, Austin TX

³ Signature Science, LLC, 1670 Discovery Drive, Charlottesville VA

⁴ Fraunhofer USA Center Mid-Atlantic CMA, Riverdale, MD, USA

⁵ Department of Computer Science, University of Maryland, College Park, MD

⁶ Department of Electrical and Computer Engineering, Rice University, Houston, TX

Abstract

Modern benchtop DNA synthesis techniques and increased concern of emerging pathogens have elevated the importance of screening oligonucleotides for pathogens of concern. However, accurate and sensitive characterization of oligonucleotides is an open challenge for many of the current techniques and ontology-based tools. To address this gap, we have developed a novel software tool, SeqScreen, that can accurately and sensitively characterize short DNA sequences using a set of curated Functions of Sequences of Concern (FunSoCs), novel functional labels specific to microbial pathogenesis which describe the pathogenic potential of individual proteins. We show that our ensemble machine learning model after training on these curations can label sequences with FunSoCs via an imbalanced multi-class and multi-label classification task with high accuracy. In summary, SeqScreen represents a first step towards a novel paradigm of functionally informed pathogen characterization from genomic and metagenomic datasets. SeqScreen is open-source and freely available for download at: www.gitlab.com/treangenlab/seqscreen

Introduction

Rapid advancements in synthesis and sequencing of genomic sequences and nucleic acids have ushered in a new era of synthetic biology and large-scale genomics. While the democratization of reading and writing DNA has greatly enhanced our understanding of large-scale biological processes¹, it has also introduced new challenges². These include use of novel DNA synthesis strategies for potentially harmful applications either by accident or intentionally, posing significant biosafety and biosecurity risks³. Previous work in which poliovirus cDNA⁴ and the 1918 Flu virus⁵ were synthesized in the absence of a template illustrate the possibility of making infectious agents purely through biochemical means. In addition to synthesized pathogens, the diversity of naturally evolving and emerging pathogenic sequences also obscures such analysis. Some contributing factors to the aforementioned analysis include the role of abiotic and environmental stress response genes

in virulence, presence of seemingly pathogenic sequences in commensals, host-specific pathogen virulence, and interplay of different genes to generate pathology³. Accurate and sensitive detection of pathogenic markers has also been confounded by the difficulty of characterizing multifactorial microbial virulence factors in the context of the biology of the host⁶. The limited number of publicly available databases to annotate and identify specific pathogenic elements within sequencing datasets further exacerbates the problem. Thus, there exists a need in the community for a tool that can accurately characterize genomic sequences in the context of functional pathogen detection and identification, thereby sensitively capturing sequences of concern (SoCs) in each sample³.

Due to difficulties with automated annotations and the lag between experimental results and sequence annotations, identifying sequences involved in pathogenesis is an ongoing challenge⁷⁻⁸. Gene Ontology (GO) terms were not designed to solely capture the nuanced biological processes and molecular functions specific to pathogens, and the pathogenesis GO term (GO:0009405) was recently scheduled for obsolescence, with the final notice given in March 2021 (<https://github.com/geneontology/go-annotation/issues/3452>). In its absence, there is no way to recognize the pathogenic possibilities of >275K UniProt accessions. Tremendous recent progress has been made with respect to taxonomic classification and pathogen characterization from isolates and metagenomic datasets. However, all existing methods either: i) assume the presence of the entire genome, ii) ignore functional information, or iii) are ill-equipped to analyze individual short sequence lengths typical of synthesized oligonucleotides (Table 1). For example, the current best practices recommendation for oligonucleotide screening by The International Gene Synthesis Consortium (IGSC) focuses solely on the presence or absence of BSAT select agents⁹. Previous benchmarking studies on microbial identification from metagenomes have shown that there exists a crucial tradeoff between taxonomic resolution and accuracy given the current state-of-the-art tools¹⁰. While modern synthetic biology and computational methods have made it possible to design and synthesize a wide variety of custom DNA^{11,12}, there exists a gap in annotation frameworks able to accurately identify known and emerging pathogens from short oligonucleotides¹³.

Recent studies have shown the potential of using k-mer based probabilistic models leveraging k-mer genotyping and logistic regression analysis to identify k-mers indicative of antibiotic resistance¹⁴. Other tools incorporating statistical frameworks for predicting markers of pathogenicity from sequencing data include PathoScope^{15,16} and SURPI¹⁷. The former utilizes sequence quality and mapping quality as parts of a Bayesian model to rapidly compute posterior probabilities of matches against a database of known biological agents, while the latter uses either Scalable Nucleotide Alignment Program (SNAP)¹⁸ based alignments to bacterial or viral databases and in some cases RAPSearch¹⁹ for more sensitive identification. Both tools also had separate releases, Clinical PathoScope²⁰ and SURPI+²¹, specifically focused on pathogen characterization from clinical samples. Another k-mer based tool by CosmosID²², precomputes reference databases (reference genomes as well as virulence and antimicrobial resistance markers) to create a phylogeny tree of microbes as well as variable-length k-mer fingerprint sets for each branch and leaf of the tree. Sequencing reads are then scanned against these unique fingerprint sets for detection and taxonomic classification. The statistics derived are then refined using predefined internal thresholds and statistical scores to exclude false positives and fine grain taxonomic and relative abundance estimates. Evaluations of this approach have shown that CosmosID achieves a high level of sensitivity in antibiotic resistance gene detection for predicting

staphylococcal antibacterial susceptibility²³; however, this is not an open-source tool and was not further evaluated in this study.

Previously, we introduced a proof-of-concept framework²⁴ for robust taxonomic and functional characterization of nucleotide sequences of interest. Here, we build upon the earlier framework and present a robust and comprehensive tool based on ensemble machine learning and functions of sequences of concern (FunSoCs) for pathogen identification and detection. Our system, SeqScreen, combines alignment-based tools, ensemble machine learning classifiers, curated databases, and novel curation-based labelling of protein sequences with pathogenic functions, to identify sequences of concern in high throughput sequencing data. Through careful, manual assignment of pathogenic functions based on published investigations of each sequence, SeqScreen depends on high quality training data to predict FunSoCs accurately. SeqScreen aspires to be the first tool to combine human interpretability and machine learning-based classification in a human-in-the-loop construct to provide a holistic solution towards classifying pathogens and offers a novel functional framework for pathogen identification in contrast to existing tools (Table 1.).

Results

Functional Benchmarking

Recent studies have underlined the significance of accurate functional annotation in various biological^{25,26}, pathological^{27,28}, and drug design^{29,30} applications. Though advances have been made to label protein sequences with corresponding GO terms, this task remains a challenging problem especially for shorter sequences. To assess the ability of SeqScreen to accurately annotate proteins and short sequences, we analyzed the performance of SeqScreen on 250 proteins from the CAFA 3³¹ training datasets. All the proteins chosen for benchmarking had associated FunSoC labels and hence were sequences containing markers considered to be harmful to humans by a panel of subject matter experts. In addition to full-length sequences, we also looked at protein fragments of four different lengths (34, 50, 67 and 80 amino acids) sampled from the same set of 250 proteins. For the purposes of this benchmarking experiment, we compared against three other functional annotation tools shown to do well in previous CAFA competitions and other benchmarking studies, namely PANNZER2³², eggNOG-mapper³³ and DeepGOPlus³⁴. It is important to note that these tools were developed to annotate unknown full-length protein sequences, and, to our knowledge, no other leading tools have been developed to assign GO terms to short protein subsequences. From the CAFA study we only considered those tools that are available to be run as command line interfaces, similar to SeqScreen, and hence omit purely web-based servers even if they were amongst the top performers in that competition (ex: NetGO³⁵, INGA 2.0³⁶). Both DeepGOPlus and PANNZER2 also outputted confidence values along with GO terms. We set the lower threshold of confidence values to consider as 0.1 after a sweep of all values to determine the one with the best performance. For the full-length sequences, Fig. 1 illustrates the results obtained on this dataset. SeqScreen had the highest precision among all the tools considered in the benchmarking study. We also observed

that, although DeepGOPlus and PANNZER2 had lower precision than SeqScreen, they had higher recall. The performance of eggNOG-mapper on complete sequences was slightly better than on subsequences.

For the partial sequences (34 aa, 50 aa, 67 aa, and 80 aa) sampled from full-length proteins, we evaluated SeqScreen's performance versus the CAFA 3 top performer. Over all four sub-lengths of the proteins, SeqScreen had the highest F1 score (Fig. 2). For the 34 amino acid length case, both DeepGOPlus and eggNOG-mapper had poor precision (0.76 and 0.38 respectively) compared to the rest of the tools. PANNZER2 had the highest recall of all the tools and the second best F1 score behind SeqScreen. All tools besides eggNOG-mapper demonstrated better recall than precision. As we increased the length to 50 amino acids, eggNOG-mapper showed the most improvement in terms of precision and recall, increasing from 0.38 to 0.69 and 0.11 to 0.40 respectively, though it still had lower accuracy than the other three tools. DeepGOPlus also showed an improvement in precision from 0.76 to 0.82. At length 67 amino acids, PANNZER2's recall remained the best among the tools whereas its precision dropped from 0.93 to 0.92. Also, DeepGOPlus's precision starts to pick up, increasing from 0.82 to 0.91. Moving from 67 to 80 amino acids, a major change was observed as DeepGOPlus attained a higher precision than PANNZER2 (0.95 compared to 0.91) and marginally surpassed PANNZER's F1 score (0.952 compared to 0.945). The recall of all the tools increased at 80 amino acids length compared to 67 amino acids.

Machine Learning - FunSoC Predictions

FunSoCs encompass sequences involved in the mechanisms of microbial pathogenesis, antibiotic resistance, and eukaryotic toxins (e.g., arachnids, cnidarians, insects, plants, serpents) threatening to humans, livestock, or crops. We identified 32 groups of sequences that could be categorized under the FunSoC framework (Supplementary Table S1) that each protein could potentially be assigned to, thereby indicating pathogenicity. We decided to formulate this as a multi-class, multi-label (i.e., each protein/sequence can be associated with one or more of the 32 FunSoCs) ML classification problem. In order to annotate potentially large numbers of query sequences with FunSoCs, we reasoned that utilizing a lookup table containing pre-predicted FunSoC labels (obtained from the ML models) for the proteins in the UniProt database would enable efficient extraction of labels for corresponding hits from the query to the table. Towards this, we tested 10 ML models based on three different strategies that use different feature selection criteria as well as a two-step pipeline that aims to filter proteins that are not associated with any FunSoCs. These models were trained on proteins manually curated and labelled with FunSoCs. For the purposes of our discussion, we show the top three performing models. To gain a more nuanced understanding of the models' performances, we considered the average precision and recall of the models on the positive labels specifically, i.e., proteins that were labelled with a "1" (minority class) for a particular FunSoC. This is an important measure to understand how well they learn to predict the minority positive class given the data imbalance which mirrors a practical application of SeqScreen where the expected number of non-pathogenic sequences in a sample is larger than specific pathogenic markers. Our test splits were reflective of this imbalance, for example, the test split for the FunSoC *virulence activity* had 23292 samples labelled "0" and 29 samples labelled "1". Table 2 shows the results of different models for each of the metrics. Although the accuracy of the methods is similar, we observed significant differences in the positive label precision and recall. Two Stage Detection + Classification Neural Networks (TS NN) and Two Stage Detection + Classification Balanced

Support Vector Classifier (TS Bl.SVC) represented two different ends of the spectrum of precision and recall, the former being more precise (P: 0.88, R: 0.69) and the latter being more sensitive (P: 0.73, R:0.88). We also found that Balanced Support Vector Classifier + Neural Network Classification using Oversampling (Bl. SVC+NN(OS)) represented an intermediate version of the other two models with precision and recall being more balanced (P: 0.87, R: 0.81). The majority vote classifier built on these three classifiers to provide a further improvement in the specificity with a slight loss in terms of recall (P: 0.90, R: 0.82). To get a more detailed perspective of the performance of the models on each of the FunSoCs, we plotted the positive label precision and recall per FunSoC. As seen in Fig. 3, the Majority Voting classifier combined the strengths of these individual classifiers to balance precision and recall across these FunSoCs.

Use case #1: Screening for known pathogens

We first present three pairs of hard-to-distinguish bacteria that often confound current metagenomic classification tools to show how SeqScreen analyzes and distinguishes hard-to-classify pathogens. Fig 4. describes the FunSoCs found to be associated with each of the eight bacterial isolate genomes. All isolates showed presence of different antibiotic resistance genes, indicating their ubiquitous presence in most bacteria. In Fig. 4 (a,b) we show a comparison of the commensal strain of *E. coli K-12 MG1655* versus the pathogenic strain *E. coli O157:H7*. The two strains showed presence of four FunSoCs, namely *cytotoxicity*, *secreted effector*, *secretion*, and *antibiotic resistance*. SeqScreen was able to accurately predict the additional presence of *Shiga toxin subunit B (stxB)*³⁷ in pathogenic *E. coli O157:H7* with the *cytotoxicity* FunSoC and differentiate it from *E. coli K-12 MG1655*. In addition, *E. coli O157:H7* also showed the presence of the *secreted effector protein EspF(U)*, which was labelled with the *secreted effector* and *virulence regulator* FunSoCs. Another example is shown in Fig. 4 (c,d) where *Clostridium botulinum* and *Clostridium sporogenes* are shown to be differentiated by four specific FunSoCs associated with *C. botulinum*. Though the organisms have a high degree of overall sequence similarity, *C. botulinum* contains the *BotA* toxin which is absent from *C. sporogenes*. We observed the presence of four FunSoCs associated with *C. botulinum*, which included *disable organ*, *cytotoxicity*, *degrade ecm* and *secreted effector* associated with hits to the *BotA* and *neurotoxin accessory protein (orf-X2)* genes, indicating the presence and the successful detection and annotation of pathogenic genes in *C. botulinum*. In contrast, *C.sporogenes* showed a unique hit to the *secretion* FunSoC, while both organisms were marked with a hit to the *bacterial counter signaling* and *antibiotic resistance* FunSoCs. Fig. 4 (e,f) shows that FunSoCs can also be used to differentiate between *Streptococcus pyogenes* (Group A Streptococcus, causative agent of Strep throat) and *Streptococcus dysgalactiae* (Group C/G Streptococcus), a near neighbor with pathogenic potential. *S. pyogenes* had the *streptopain (speB)* and *exotoxin type H (speH)* genes associated with the *induce inflammation* FunSoC, whereas *S. dysgalactiae* had the *immunoglobulin G-binding protein (spg)* gene with the *counter immunoglobulin* FunSoC, thereby differentiating it from *S. pyogenes*. Both bacteria showed presence of *cytotoxicity*, *secretion*, and *antibiotic resistance*. In addition to pathogens, we show in Fig. 4 (g,h) that the FunSoC based framework can also capture well-characterized commensals like *Streptococcus salivarius* and *Lactobacillus gasseri*. We see that both these bacteria reported the least number of FunSoCs, validating the negative control experiment. *S.salivarius* contained a hit the *secretion* FunSoC

from genes encoding competence proteins. In differentiating near neighbor pathogens, SeqScreen selectively annotated regions in genomes that contributed to pathogenicity across various categories.

In addition to FunSoCs assignments, we evaluated how existing alignment approaches handle the identification of pathogen near neighbors. To motivate our experiments, we initially considered the widely used BSAT list to triage isolates (see Methods section on SeqMapper), as it is representative of a current strategy for pathogen screening approaches in the DNA synthesis industry. We mapped *C. sporogenes* (SRR8758382) reads against the BSAT database using the Bowtie2 module of the SeqMapper workflow, and 98.28% of the reads hit to *C. botulinum*. The high percentage of hits to *C. botulinum* underlines the shortcoming of simplistic triaging methods to accurately differentiate between near neighbors and pathogens. We further considered popular taxonomic classifiers to analyze how accurately near neighbor pathogens were separated. We compared the results of six different tools, Mash dist³⁸, Sourmash³⁹, PathoScope^{15,16}, Kraken2⁴⁰, MetaPhlAn2⁴¹, KrakenUniq⁴² and Kaiju⁴³, with the following three pairs of near-neighbors and pathogens: *E. coli* K-12 MG1655 and *E. coli* O157:H7, *C. sporogenes* and *C. botulinum*, and *S. dysgalactiae* and *S. pyogenes*. Table 3 shows the results of running the taxonomic tool on these bacteria with their complete databases and the top hits for each are reported. Strain level differences between the two *E. coli* near neighbor was hard for almost all the tools to distinguish. Kaiju and MetaPhlAn2 could only predict *E. coli* at species level for both strains, and since those tools were designed to only report down to the species level, strain-level pathogenicity will always be missed. Kraken2 incorrectly predicted non-pathogenic *E. coli* K-12 MG1655 as the pathogenic strain *E. coli* O157:H7. PathoScope and KrakenUniq incorrectly predicted the non-pathogenic *E. coli* K-12 MG1655 strain as *E. coli* BW2952 and *E. coli* O145:H28. Mash dist and Sourmash were the only tools that reported the true *E. coli* K-12 strain. The tools performed considerably better when predicting for *E. coli* O157:H7, as Mash dist, Sourmash, PathoScope, Kraken2 and KrakenUniq were able to predict the strain correctly. When considering the two *Clostridium* near neighbors, PathoScope, Kraken2 and KrakenUniq misclassified *C. sporogenes* as *C. botulinum*. In contrast, *C. botulinum* was incorrectly called *C. sporogenes* by Mash dist, Sourmash and MetaPhlAn2. While predicting for the *Streptococcus* near neighbors, all tools predicted *S. pyogenes* correctly and only PathoScope misclassified *S. dysgalactiae* as *S. pyogenes*, while other tools called it accurately. In summary, our experiments demonstrated that none of the tools were able to correctly predict all pathogens and near neighbors at the species and strain levels. SeqScreen provides a more detailed framework beyond species or strain-level taxonomic classifications to aid the user in interpreting the pathogenicity potential of a query sequence, including exact protein hits, GO terms, multiple likely taxonomic labels with confidence scores, and FunSoC assignments.

Use case #2: Screening for novel pathogens

To highlight the advantage of using SeqScreen's FunSoC based pathogen detection pipeline in contrast to relying on taxonomic labels we evaluated how the absence of the exact set of species or strain entries in the database corresponding to the bacterial genome query would impact the classifications by these tools. This was done to simulate a query of a novel pathogen genome by removing the entries corresponding to the query bacterial genome from the database. We chose two tools for this experiment, Mash dist and PathoScope, as modifying their databases for this experiment was readily achievable

and both performed well in the previous use case. Table 4 shows the results of the classifiers using these modified databases. As expected, the closest near neighbor of the query genome is selected when a pathogen is not present in the database, which while representing the expected behavior, is not suitable for sensitive flagging of pathogenic sequences. As is the case with the complete databases, both the tools misclassified the *E. coli* strains with PathoScope only being able to classify *E. coli K-12 MG1655* at species level and Mash dist instead reporting a hit to the pathogenic *E. coli O16:H48* strain. For the *Clostridium* species, both the tools called the pathogen as its non-pathogenic near neighbor, emphasizing the difficulty of identifying these pathogens in a simulated novel pathogen environment. In the case of *Streptococcus*, *S. dysgalactiae* was classified as *S. sp. NCTC 11567* by Mash dist and *S. intermedius* by PathoScope, whereas *S. pyogenes* was classified as its near neighbor *S. dysgalactiae* by Mash dist and *S. infantarius* by PathoScope. In contrast, as seen in Fig. 4, retaining genus specific hits from SeqScreen was sufficient to observe functional differences between the near neighbor pathogens. This experiment showed that current approaches may still fail to separate near neighbor pathogens and hence a novel FunSoC-based functional framework could help fill the gap and capture sequence level pathogenic markers.

Use case #3: Screening human clinical samples for an unknown pathogenic virus

To further illustrate SeqScreen's ability to identify pathogenic sequences in clinical samples, we ran SeqScreen on the sequencing data obtained from the peripheral blood mononuclear cells (PBMC) of three COVID-19 patients and three healthy patients as reported in the study by Xiong et al⁴⁴. We reasoned that the samples from COVID-19 patients should contain certain reads with functional markers that would indicate presence of the SARS-CoV-2 virus. To better understand SeqScreen's application in analyzing clinical samples for unknown pathogenic viruses, we chose to run an older version of SeqScreen (v1.2) on these samples, retaining the same analysis functionality with a database that predated the COVID-19 pandemic and the inclusion of SARS-CoV-2 virus. This was done for two main reasons. First, we wanted to evaluate SeqScreen's ability to retrieve functional pathogenic information by simulating an experiment with an unknown virus along with a database that did not contain the causative virus. Second, we wanted to highlight SeqScreen's ability to detect GO terms and FunSoCs directly from metatranscriptomes of clinical samples with low levels of the novel pathogen. For this study, we focused on GO terms that were specific to the COVID-19 samples and viral proteins (i.e., GO terms that were not assigned to bacterial, eukaryotic, or archaeal proteins or observed in the healthy controls). Only three GO terms met these criteria within one of the COVID-19 samples (CRR119891). All three of the GO terms, suppression by virus of host ISG15 activity (GO:0039579), induction by virus of catabolism of host mRNA (GO:0039595), and suppression by virus of host NF-kappa B transcription factor activity (GO:0039644) were indicative of SARS-CoV-2 virus activity. SeqScreen assigned replicase polyprotein 1ab from Bat coronavirus 279/2005 (UniProt ID: P0C6V9, e-value: 5.8e-29) to one sequence read and reported these three GO terms in sample CRR119891. Searching for other coronavirus taxonomic assignments in that sample revealed one additional read that SeqScreen assigned to spike glycoprotein from Bat coronavirus HKU3 (UniProtID: Q3LZX1, e-value: 1.3e-09). No other coronavirus reads were identified in the samples, consistent with the report from the original publication in Xiong et al⁴⁴ that very few to no SARS-CoV-2 reads were identified in the PBMC samples. In the SeqScreen v1.2 database, the associated FunSoC with the replicase polyprotein 1ab was evasion and the FunSoCs predicted for the spike protein were adhesion and invasion, which reflect the biological functions of the two proteins and indicate

presence of virulence. To compare SeqScreen v1.2 results to another tool, we ran HUMAnN2⁴⁵ on the six PBMC metatranscriptomes to check for presence of virulence markers and pathways. The HUMAnN2 results did not point to any evidence for presence of COVID-19 specific markers in this sample nor the others (Supplementary Data S1), which is expected given the focus of the tool on reporting enriched genes and pathways, rather than rare pathogenic sequences. As SeqScreen extensively characterizes individual short protein-coding sequences and is geared towards identifying functional markers of pathogenicity, it can sensitively detect trace amounts of pathogenic signal in clinical samples.

Discussion

The performance of SeqScreen on a wide variety of benchmarking and real datasets highlights SeqScreen's utility for pathogen characterization of short sequences. One fundamental result of this study is SeqScreen's demonstrated ability to provide functional annotations of partial protein sequences with high accuracy. While annotating full-length sequences, SeqScreen showed high levels of precision amongst all benchmarking datasets but DeepGOPlus and PANNZER2 had higher levels of recall indicating that, though precise, SeqScreen is selective in its annotation. We showed that SeqScreen has better precision on shorter sequences than current functional annotation tools and on a subset of data obtained from the CAFA 3³¹ challenge. We also established that our machine learning models can learn the underlying GO term annotations and keywords associated with proteins and annotate protein-coding sequences with FunSoCs.

Determining the potential for pathogenicity only from information contained in UniProt is challenging because most of the sequences that mediate pathogenicity are under-annotated or unannotated. Existing GO terms are not particularly apt for describing parasitism as practiced by bacterial, fungal, and protozoan pathogens. In contrast, many GO terms specify how viruses parasitize host cells. In general, the viral sequences in UniProt appeared to be of a higher annotation quality than those of other parasites. However, one issue with many of the sequences from RNA viruses is that they are represented only as parts of polyproteins. The GO term and keyword annotations in UniProt are assigned to the entire polyprotein, which prevents the evaluation of the constituent protein functions. For our purposes, we found that the best annotated sequences of concern in UniProt were the eukaryotic toxins that affected mammals⁴⁶. The "toxin activity" GO term designation can be problematic for the uninitiated because of its lack of specificity. For example, a toxin may only be toxic for invertebrates or plants. Plasmid toxins of the toxin/antitoxin system are only toxic to bacteria, but they are numerous in sequence databases and can be reported in generic searches for "toxins"⁴⁷. To distinguish these, we found the UniProt keywords that subclassify toxins to be particularly helpful.

A novel feature of SeqScreen for pathogen detection and characterization is the addition of FunSoCs as a labeling system for each sequence in the query. FunSoCs are molecular activities of pathogens that contribute to its pathogenesis in human, crop, or livestock hosts. Using controlled vocabularies and other data mined from popular protein databases, we showed that our models can capture FunSoCs with a high level of precision. To improve the balance between precision and recall over most of the FunSoCs, we proposed a majority voting ensemble classifier. SeqScreen utilizes a lookup table created by

classifying all UniProt⁴⁸ proteins using the ensemble classifier to annotate query sequences with FunSoCs. SeqScreen's FunSoC biocurations are not the first attempt to collate sequences of concern in a specific computational framework and/or database. Prior efforts such as the Virulence Factor Database (VFDB)⁴⁹, Pathosystems Resource Integration Center (PATRIC)⁵⁰, and Pathogen-Host Interaction database (PHI-base)⁵¹ all offer resources for identification of virulence factors and pathogenic sequences. VFDB is a database of virulence factors that have been widely used⁵² but is limited due to many of the sequences not having clearly available annotations or justification for their pathogenic status. PATRIC primarily focused on annotation of isolates/pathogens but not individual sequences, and PHI-base describes the pathogen-host interactions but does not focus on pathogenic effects on the host. SeqScreen was designed to specifically overcome some of the major aforementioned limitations through an iterative ensemble learning framework that leverages functional information combined with biocurations to identify FunSoCs

The challenge of pathogen identification and detection from sequence level features is significant and requires a careful, nuanced approach. A given species may include both pathogenic and non-pathogenic strains. These may not be well-defined by taxonomic considerations⁶, since sequences with similar taxonomic labels may contain pathogenic elements as well as non-pathogenic markers. In our work, we showed that sequences annotated with a subset of high-confidence FunSoCs can be analyzed to detect pathogenic presence in the sample. Taxonomic classifiers often are ambiguous about similar pathogens and near neighbors within the same genus or species, such as commensal *E. coli K-12 MG1655* and pathogenic *E. coli O157:H7*, as well as *C. botulinum* and *C. sporogenes*, and *S. dysgalactiae* and *S. pyogenes*. We show that FunSoCs can be used as unique signatures to distinguish these pairs. We also saw that commensal bacteria such as *L. gasseri* had no FunSoCs associated with it, other than antibiotic resistance, validating our negative control and highlighting SeqScreen's ability to accurately identify commensals. Note, several the commensals analyzed in this study contain genes that can cause infection in humans, but these microbes are rarely disease-causing agents.

Our experimental results underscore the importance of using a function-based framework in contrast to the prevailing taxonomy-based classifiers and pathogen detection tools. SeqScreen's FunSoC based pathogen detection approach is sensitive to specific gene-based differences between closely related strains and accurately identifies pathogenic markers. Out of the tools we evaluated, only Kaiju was able to accurately distinguish all the near neighbors from pathogens at the species level. The protein-based classification strategy used by Kaiju is different from other k-mer based tools, but similar to SeqScreen's functional based characterization framework, indicating the advantages of using the functional units in proteins to identify pathogens. SeqScreen provides an advantage in that it also reports the most likely strain-level assignments and protein-specific functional information for each sequence, including GO terms and FunSoCs, to accurately identify pathogenic markers in each sequence without relying solely on taxonomic markers. Though it was not created to be a taxonomic classifier, SeqScreen's performance on taxonomy can be found in Supplementary Data S2, S2.2 and Supplementary Table S2. We also observed through inspecting the FunSoC lookup table that SeqScreen preserves FunSoC labels even when the proteins are distantly related (up to 40% sequence similarity). Hence, the FunSoC abstraction represents a robust framework to detecting novel pathogens as it does not rely on specific taxonomic labels in the database but on learning latent features that connect similar pathogenic makers. SeqScreen also provides a more detailed framework

beyond species or strain-level taxonomic classifications to aid the user in interpreting the pathogenicity potential of a query sequence, including exact protein hits, GO terms, multiple likely taxonomic labels with confidence scores, and FunSoC assignments.

The task of mapping biological (e.g., functional annotations) and textual features (e.g., keywords and abstract metadata) to these FunSoCs is non-trivial for three reasons. The first concerns identifying from the literature a sufficiently large training set of sequences associated with each FunSoC. Second, variability in annotation across subject matter experts and inconsistencies in database annotations often makes it challenging to incorporate relevant features. Third, the amount of labelled data available per FunSoC is disproportionate which makes accurate multi-label and multi-class classification difficult. Also, the positive labels are far fewer when compared to the negative labels making the accurate prediction of positive labels non-trivial due to class imbalance.

One known limitation of SeqScreen is that it heavily depends on annotated sequences for identification of FunSoCs. As of April 2021 (UniProt release 2021_02), there are 1.5 million proteins with evidence at the protein or transcript level (less than 0.75%), with 64 million proteins with functions inferred from homology and over 212 million proteins total. Through multiple years of biocuration efforts, our team was able to characterize thousands of proteins specific to pathogenic function, augmenting information contained in UniProt, and enabling robust pathogenic sequence screening of sequences of high concern. However, coordinated community efforts are needed to further extend out and improve annotation quality of proteins in these key databases. We also note that while we have shown SeqScreen to be an accurate pathogen detection tool, explicitly identifying and labelling pathogens is not possible with only FunSoC information, as seen in Fig. 4, and the presence of genes underlying the FunSoC annotations should be considered when interpreting results. SeqScreen identifies and flags sequences having functions of concern (or FunSoCs) but stops short of performing pathogen identification, as it was designed to only characterize individual DNA sequences. In future work, we aim to extend our FunSoC-based machine learning (ML) framework towards pathogen identification by analyzing sequences at the whole genome level.

Finally, while SeqScreen can accurately screen oligonucleotides and short DNA sequences for FunSoCs, large metagenome-scale pathogen analysis is still an open challenge. Currently, the accuracy and sensitivity of SeqScreen annotation comes at a substantial cost of runtime and memory requirements compared to other tools and pipelines. To address this, one possible solution is to use a read or database subsampling method such as RACE⁵³ that may be able to preserve the full complement of taxonomic and functional diversity while drastically reducing runtime.

In conclusion, SeqScreen describes a novel, comprehensive sequence characterization and pathogen detection framework based on a multimodal approach that combines conventional alignment-based tools, machine learning and expert biocuration to produce a new paradigm for novel pathogen detection tools beneficial to both synthetic DNA manufacturers and microbiome scientists alike. SeqScreen is the first open-source, modular framework for transparent and collaborative research to improve DNA screening practices beyond simple screens against BSAT agents and toxins.

Methods

Pipeline Overview

The SeqScreen pipeline was built using Nextflow⁵⁴, a domain-specific language for creating scalable and portable workflows. SeqScreen combines various stages in separate Nextflow modules and is available as an open-source tool on bioconda (<https://anaconda.org/bioconda/seqscreen>). The modular nature of the pipeline offers advantages in terms of ease of updating or replacing specific software modules in the future versions if new bioinformatics tools and databases are shown to outperform its current modules and workflows. SeqScreen accepts nucleotide FASTA files as input, assuming one protein-coding sequence is present within each query sequence of the FASTA file. Each input file is verified for the correctness of the FASTA format and then passed on to the initialization workflow in *sensitive* mode, which first converts ambiguous nucleotides to their corresponding unambiguous options and performs six-frame translations of nucleotide to amino acid sequences for input into downstream modules like RAPSearch2¹⁹, which accepts amino acid sequence as input. After initialization, the sequences pass through various downstream modules that add taxonomic and functional annotations to the sequences that inform its FunSoC assignment. Fig. 5 illustrates the various modules and workflows in SeqScreen. SeqScreen can be run in two different modes - *fast* mode and *sensitive* mode. The *fast* mode runs a limited set of pipelines that are tuned to rapidly annotate sequences in an efficient performance-centric approach. The *sensitive* mode (using the `--sensitive` flag) uses much more accurate and sensitive BLASTN-based alignments and outlier detection⁵⁵ steps for taxonomic characterization. Further, for sensitive functional annotations it uses BLASTX to identify hits to the curated UniRef100 database. All analyses in this study were performed with SeqScreen fast mode, other than the SeqMapper-focused analysis that was run in sensitive mode.

SeqMapper

The SeqMapper workflow is part of the *sensitive* mode of SeqScreen and aims at detecting Biological Select Agents and Toxins (BSAT) sequences through efficient sequence alignment methods. We use a two-pronged approach by analyzing both the nucleotide and amino acid sequence alignments to BSAT reference genomes using Bowtie2⁵⁶ and RAPSearch2¹⁹, respectively. While this workflow is only limited to reporting hits to BSAT genes and proteins, downstream workflows are used to capture and collate whether a gene is of interest at a functional level (e.g., functional differentiation between BSAT housekeeping and toxin hits are not delineated at this step). This workflow is sensitive to detect BSAT sequences, but not precise in differentiating BSAT sequences from their near neighbors. In addition to the above databases, users can also optionally obtain other features of interest, such as HMMs identified by HMMER⁵⁷ from Pfam⁵⁸ proteins by using the optional HMMER module in SeqScreen. The BSAT sequences were primarily derived from the following website:

<https://www.selectagents.gov/sat/list.htm> and the full contents of the BSAT bowtie2 database is available at: <https://rice.box.com/s/6c5x10qcu66xbuf3n8yp4fkf9cfwn3wv>.

Taxonomic Classification

In the taxonomic classification workflows for both *fast* and *sensitive* modes we rely on widely used state-of-the-art alignment-based tools to classify sequences. SeqScreen obtains alignments to both DNA and amino acid databases. While aligning to amino acid databases provides taxonomic information as well as functional information, aligning to nucleotide databases provides additional sensitivity, especially for non-coding regions. The taxonomic classification module for *fast* mode is an ensemble of DIAMOND⁵⁹ and Centrifuge⁶⁰, two established and widely used tools for protein alignment and taxonomic classification. First, DIAMOND is used to align the input sequences to a reduced version of the UniRef100 database. DIAMOND is an open-source software that is designed for aligning short sequence reads and performs at approximately 20,000 times the speed of BLASTX with similar sensitivity. Our reduced version of the UniRef100⁶¹ database only contains proteins with a high annotation score. Not including poorly annotated proteins both decreases the runtime and increases the specificity of SeqScreen functional annotations. SeqScreen then runs Centrifuge, a novel tool for quick and accurate taxonomic classification of large metagenomic datasets. Centrifuge classifications are given higher weights and are always assigned a confidence score of 1.0. SeqScreen always picks the taxonomic rank with the highest score for Centrifuge and assigns it to the sequence. In the case where Centrifuge fails to assign a taxonomic rank to a particular sequence, we assign DIAMOND's predictions to it. To incorporate DIAMOND's predictions, we consider all taxonomic ids that are within 1% of the highest bit-score as the taxonomy labels for a sequence (Supplementary Figure S1). The *sensitive* taxonomic classification workflow uses BLASTX and BLASTN for aligning to amino acid and nucleotide databases, respectively. For BLASTX, we again use our reduced version of the UniRef100 database (Supplementary Data S3). BLASTN results are processed through outlier detection to identify which of the top hits are significantly relevant to the query sequence. The *sensitive* mode parameters are set so that if a cut is made, all hits above the cut line are returned; otherwise, all hits are returned. All hits within the outlier detection cutoff (BLASTN) or within 1% (sensitive parameter cutoff=1) of the top bitscore will be saved as the top hits for a given query sequence. Next, all hits reported by BLASTN and BLASTX are sorted by bitscore and listed for a query. Taxonomic IDs are ordered so that BLASTN are reported first, followed by BLASTX. Order-dependent taxonomic assignments will then be based on the first taxonomic ID reported (typically BLASTN hit). Default E-values (--evalue) and max target seqs (--max_target_seqs) for BLASTN and BLASTX are set to 10 and 500, respectively. Since both parameters limit the number of matches to the query sequence, modification of these parameters may be necessary for short and ubiquitous sequences. For BLASTN and BLASTX, the reported confidence values are based on bitscores (bitscore / max bitscore), as inspired by orthology estimation⁶².

Functional Annotation and FunSoC Prediction

Using the predicted UniProt IDs and their bit scores from DIAMOND, SeqScreen obtains a list of all predicted UniProt IDs whose bit score is at most 3% less than the highest bit score and compiles all the associated GO terms for each UniProt ID.

To assign FunSoCs to each input sequence, we have developed a database which contains a mapping of all UniProt IDs to FunSoCs. The construction of SeqScreen database is described in detail in Supplementary Data S3.

Report Generation

Following the computational workflows, SeqScreen produces a tab-separated report file with the predictions of each input sequence as well as an interactive HTML report. The HTML report allows users to search and filter the results based on a variety of criteria such as FunSoC presence, GO term presence, and sequence length. The HTML report is a convenient way to browse the results of large inputs as it loads results in small chunks so that arbitrarily large results can be viewed (Fig. 6 and Supplementary Figure S2).

Functional Benchmarking

Data for the functional benchmarking was downloaded from the CAFA website (<https://www.biofunctionprediction.org/cafa/>). The CAFA 3 training data was downloaded from the website (https://www.biofunctionprediction.org/cafa-targets/CAFA3_training_data.tgz). From the training set, a subset of 250 proteins having appropriate lengths (at least 200 aa) were chosen for the benchmarking. A set of (250) proteins of sub-lengths 34 aa, 50 aa, 67 aa and 80 aa was derived from this set of proteins for sub-lengths benchmarking. To create the sub-lengths for the respective proteins, we randomly selected a starting residue from each of the 250 proteins and considered the stretch of residues up to the desired lengths as the sub-protein. The proteins were then run through each of the tools: PANNZER2³², eggNOG-mapper³³ and DeepGOPlus³⁴. Further details about the dataset, tools and commands and databases the tools were run with are shown in the Supplementary Data S2, S2.1 and Supplementary Table S2.

Ensemble Machine Learning for FunSoC Prediction

One of the major applications of SeqScreen is its ability to combine functional and taxonomic information for pathogen detection. To assign pathogenic functions to query sequences in each sample, SeqScreen labels relevant sequences with FunSoCs. Each FunSoC captures a process contributing either to pathogenesis or countermeasure resistance. Proteins representing the FunSoCs were identified primarily through literature review with some database perusal (VFDB⁴⁹, PHI-base⁵¹). The expert human biocurators developed queries using terms from controlled vocabularies and in specified UniProt fields to obtain sequence sets for each FunSoC. Examples of UniProt queries are provided in Supplementary Data S4. After initial formulation with UniProt queries, the biocurator FunSoC annotations were verified through manual literature reviews thereby maximizing the number of sequences specific to the FunSoC category while eliminating false positives. An updated database of SeqScreen biocurated FunSoCs is maintained in Supplementary Data S5. The proteins of each FunSoC were then used as a training set. The training set sizes for each FunSoC ranged from 4,722 for *disable organ* to 24 for *counter immunoglobulin*. These also included proteins that had annotation scores less than 3, which were pruned out in the preprocessing step to get high-quality labelled training data. We used these proteins as the training dataset for our Machine Learning models to capture underlying mappings between the sequence features and FunSoCs. Each of the curated proteins

is assigned a binary label for each of the 32 FunSoCs. This can be visualized as a matrix M where an entry m_{ij} marked as 1 represents that Protein_{*i*} is annotated as having FunSoC_{*j*}, or in other words Protein_{*i*} is positively labelled for that particular FunSoC_{*j*}. On the contrary, m_{ij} marked as 0 means that Protein_{*i*} does not belong to FunSoC_{*j*} and is negatively labelled for that FunSoC. Every sequence of the collected set of labelled proteins is positively labeled for at least one FunSoC.

Dataset Curation and Preprocessing

To build a training and testing dataset for our models, proteins were obtained that were not positively associated with each FunSoC. This was done to avoid tagging every sequence analyzed by SeqScreen with a particular FunSoC. The great majority of biological sequences are benign, so we decided to append the set of curated proteins with a selected set of proteins from SwissProt and labelled them with 0's for each FunSoC. This forced the model to learn it could neglect assigning FunSoCs to proteins. Further, these proteins were only selected if they had an annotation score greater than 3, to control for the quality of annotation. Once this set of proteins and their respective negative labels were added to the initial list of curated proteins, we extracted relevant features from each of the proteins to be included as features. GO annotations and keywords for each protein were extracted from UniProt. Once extracted, a large binary feature matrix F was constructed for the total set of proteins. The rows represent each protein in the dataset and the columns represent all possible features of the dataset, (i.e., a union of all the individual features of each protein in the dataset). Each entry f_{ij} in the feature matrix F , is a binary value representing presence or absence of a particular feature_{*j*} for a protein_{*i*}. Apart from controlling for annotation scores, to further help reduce the effect of noise and non-specific keywords or GO terms from our datasets, we decided to preprocess the feature set to exclude any sparse features that occurred in less than 10 proteins. This reduced the total number of features from over 50k to around 16k features. This was the final feature matrix used for downstream Machine Learning tasks.

Machine Learning Models

The challenge of assigning FunSoCs to proteins is a multi-class, multi-label classification problem where a given protein can be assigned to any (or none) of 32 different FunSoCs. These are often independent of one another and can be learned individually. Multi-class and multi-label classifications are hard as often these classes have different amounts of training data available. This might make certain labels harder to predict than others and result in a poor classifier that is biased to certain well curated class labels. This also makes accuracy a tricky metric to handle given the imbalance in data labels. From our feature matrix we observed that the number of proteins labelled negatively (i.e., 0) for all FunSoCs greatly outnumbered those with at least one positive label. Though this mirrors the imbalance in real data, it poses a challenge in learning tasks as the models tend to learn features only from the majority class thereby achieving high accuracy by classifying everything as negative. To address this, we investigate incorporating class weights and sampling techniques into our models.

Recently, the explainability of predictive models for machine learning has been emphasized in microbiome research^{63,64}. To follow this idea of producing explainable results, we used feature selection or two-step modular approaches that aided the interpretability of the models. Though we analyzed 10 models for our FunSoC prediction task, here we describe the top three best-scoring approaches. The first is a two-stage modular pipeline that uses neural networks. For the purposes of this discussion, we describe stage 1 as the detection stage and stage 2 as the classification stage. In the detection stage, we use a multi-layer perceptron with one hidden layer consisting of 200 neurons. The network has a binary output which encodes whether the input sequence is associated with at least one FunSoC. Proteins without FunSoCs are eliminated from downstream classification. Proteins that have at least one FunSoC reach the classification stage which detects FunSoCs associated with a sequence in a multi-label fashion. The architecture of the detection stage consists of one hidden layer with 500 neurons. The output layer contains one neuron per FunSoC that outputs a binary label. For both detection and classification, all internal layers use ReLU activation while the output layers have sigmoid classification. The binary cross-entropy loss function is shown in Eqn. 1. where y (0 or 1) is the class label and p is the predicted probability that the observation belongs to class y . This is used in conjunction with the Adam⁶⁵ optimizer and the models also incorporate a dropout layer with rate 0.2.

$$\text{Binary cross-entropy loss: } L = - (y \log(p) + (1 - y) \log(1 - p)) \quad (1)$$

The second model is analogous to the two-stage neural network pipeline except for two major differences. First, the neural networks are replaced with Linear-Support Vector Classifiers (LinearSVC). The LinearSVCs are tuned with training label weights to account for class imbalance and have a binary output for detecting the presence of at least one FunSoC. Second, the classification architecture now consists of different LinearSVCs, one for each FunSoC. Each classification LinearSVC has a binary output indicating the presence of that FunSoC. Both the detection and classification LinearSVCs uses squared hinge loss with L1 penalty (shown in Eq. 2, where Y_i is the output label, X_i is the feature vector of sample i and β is the vector of weights, n is the number of samples and p is the number of features), a c-value (C) of 0.01 and 4000 iterations for convergence during training.

$$\text{Cost function: } L = C \sum_{i=1}^n (Y_i \max(0, 1 - \beta^T X_i) + (1 - Y_i) \max(0, 1 + \beta^T X_i))^2 + \sum_{j=1}^p |\beta_j| \quad (2)$$

The third best performing model deviates from the two-stage detection and classification pipeline and instead incorporates a feature detection step prior to classification to help with interpretability. The model is a combination of LinearSVCs and neural networks and uses one of each for each FunSoC. In the first step, LinearSVCs are used as a feature selection tool to extract important features for each FunSoC. Since the L1 penalty was used for classification, it assigns a weight of zero to features that are not discriminative towards the FunSoC classification. The LinearSVCs were also augmented with class weights to make the feature selection sensitive to the minority positive labels in each FunSoC. The LinearSVC used an L1 penalty, a c-value of 0.01 and 3000 iterations. Once the features are selected, this new feature

set is fed as an input to the neural network for classification. The neural network has one hidden layer with 100 neurons and uses ReLU activation for internal layers and sigmoid activation for the output layer, a dropout layer with rate 0.2 and binary cross-entropy loss. To further lessen the effects of class imbalance, after feature selection random oversampling of the minority class was done prior to training the neural network to balance the number of positive and negative samples in the training set.

The LinearSVCs for all the models were directly incorporated using their scikit-learn⁶⁶ implementations. To implement the neural networks, the Keras⁶⁷ package was used. Parameter tuning was carried out by varying the c-value (C) and testing using different kernels for other non-linear SVCs whereas the number of layers, depth of the neural network, activations, dropout rate, and including class weights was tested for the neural network model. The parameters reported above were consistently the best performing across the parameter space while maintaining a relatively simple architecture and were chosen as the final parameters.

To combine the strengths of all the classifiers discussed above, we also analyzed an additional model that employed an ensemble majority vote on the outputs of the three models. The ensemble classifier was developed after visualizing performances of the three individual classifiers on hard-to-classify FunSoCs like *develop in host*, *nonviral invasion*, *toxin synthase* and *bacterial counter signaling* (as seen in Fig. 3) to try and balance the disparity between precision and recall. To have a model that does not suffer from sub-optimal performances on multiple FunSoCs we reasoned that a majority vote classifier would be a better overarching model for a consistent performance across FunSoCs for downstream applications, especially pathogen detection. We choose a subset of FunSoCs having both precision and recall above 0.8 for the pathogen detection applications and being the most determinative of pathogen presence as assigned by the biocurators.

A primary focus during the development of the ML models was to make the feature selection and classification strategies as explainable as possible instead of applying it as “black box” techniques. The interpretability of the models was also imperative for iterative curation where the features and labels could be passed on to the biocurators to potentially curate and refine more examples of proteins belonging to the respective FunSoCs. These refined labels were then fed back into the ML models to obtain the final FunSoC assignments. To minimize variability of our ML results and make SeqScreen analysis more reproducible, ML-based predictions are pre-computed on all of UniProt and is included in the SeqScreen database as a lookup file. This allows users to explicitly view and check the FunSoCs associated with individual UniProt hits and corroborate their biological accuracy.

Pathogen Sequence Identification

In this work, we provide motivating experiments that underlie an important application of SeqScreen towards pathogen detection. We run SeqScreen on isolate reads obtained from four pairs of well characterized but hard-to-distinguish pathogens namely *E. coli* K-12 MG1655 and pathogenic *E. coli* O157:H7, as well as distinguishing *C. botulinum* from *C. sporogenes*, and *S. dysgalactiae* from *S. pyogenes* in addition to identifying the commensals *S. pyogenes* and *L. gasseri*. To

carry out accurate FunSoC annotations, the reads were preprocessed to remove low quality bases and adapters using Trimmomatic⁶⁸. In addition to evaluating SeqScreen, we also ran the set of bacterial reads through Mash dist³⁸, Sourmash³⁹, PathoScope^{15,16}, Kraken2⁴⁰, KrakenUniq⁴², MetaPhlan2⁴¹, and Kaiju⁴³. These tools (except PathoScope) were run as part of the MetScale v1.4 pipeline (<https://github.com/signaturescience/metscale>) using default parameters and a quality trim threshold of 30 with Trimmomatic, k value of 51 with Sourmash and all other MetScale v1.4 default parameters, tool containers, and databases for analyzing paired-end Illumina reads. We evaluated the results on their respective complete databases as well as a modified version of their database (for Mash dist and PathoScope) in which the entries corresponding to the query genome were removed to simulate a novel or emerging pathogen. In case of *E. coli* the respective strains were removed while in the case of the other bacteria the species (and all strains) were omitted from the database. To facilitate manipulating the Mash database, we created the Mash database from a new version of RefSeq (downloaded November 2020, Release 202). The RefSeq genomes were downloaded using the tool ncbi-genome-download available on conda (<https://github.com/kblin/ncbi-genome-download>)

Sequences from Peripheral Blood Mononuclear Cells in COVID-19 Patients

Sequencing data from three samples of healthy individuals (CRR125445, CRR125456, CRR119890) and three samples of COVID-19 samples (CRR119891, CRR119892, CRR119893) from the study Xiong et al⁴⁴ were considered for our analysis. After preprocessing reads through quality control and human read removal (see detailed methods here: <https://osf.io/7nrd3/wiki/home/>), each sample was passed through SeqScreen v1.2 to obtain the respective set of proteins, FunSoCs, and GO terms outputs. GO terms were parsed with the CoV-IRT-Micro scripts (<https://github.com/AstroBioMike/CoV-IRT-Micro>), and GO terms were identified that were unique to both the COVID-19 patient samples and viral proteins. The SeqScreen tsv final report was used to connect proteins to GO terms and find all coronavirus reads in the samples.

Code Availability

SeqScreen is available on GitLab at <https://gitlab.com/treangenlab/seqscreen>. SeqScreen can be installed via Bioconda:

<https://anaconda.org/bioconda/seqscreen>

References

1. Hughes, R. A. & Ellington, A. D. Synthetic DNA synthesis and assembly: Putting the synthetic in synthetic biology. *Cold Spring Harbor Perspectives in Biology* **9**, (2017).
2. *Biodefense in the Age of Synthetic Biology*. *Biodefense in the Age of Synthetic Biology* (National Academies Press, 2018). doi:10.17226/24890.
3. Leo Elworth, R. A. *et al.* Synthetic DNA and biosecurity: Nuances of predicting pathogenicity and the impetus for novel computational approaches for screening oligonucleotides. *PLoS Pathogens* **16**, e1008649 (2020).
4. Cello, J., Paul, A. V. & Wimmer, E. Chemical synthesis of poliovirus cDNA: Generation of infectious virus in the absence of natural template. *Science* **297**, 1016–1018 (2002).
5. Tumpey, T. M. *et al.* Characterization of the reconstructed 1918 Spanish influenza pandemic virus. *Science* **310**, 77–80 (2005).
6. Agents, N. R. C. (US) C. on S. M. for the D. of a G. S.-B. C. S. for the O. of S. *Sequence-Based Classification of Select Agents*. *Sequence-Based Classification of Select Agents* (National Academies Press, 2010). doi:10.17226/12970.
7. Diggans, J. & Leproust, E. Next Steps for Access to Safe, Secure DNA Synthesis. *Frontiers in Bioengineering and Biotechnology* **7**, 86 (2019).
8. Salzberg, S. L. Next-generation genome annotation: We still struggle to get it right. *Genome Biology* vol. 20 92 (2019).
9. Eisenstein, M. Synthetic DNA firms embrace hazardous agents guidance but remain wary of automated “best-match.” *Nature Biotechnology* vol. 28 1225–1226 (2010).
10. Randle-Boggis, R. J., Helgason, T., Sapp, M. & Ashton, P. D. Evaluating techniques for metagenome annotation using simulated sequence data. *FEMS Microbiology Ecology* **92**, (2016).
11. Hughes, R. A. & Ellington, A. D. Synthetic DNA synthesis and assembly: Putting the synthetic in synthetic biology. *Cold Spring Harbor Perspectives in Biology* **9**, (2017).
12. Gould, N., Hendy, O. & Papamichail, D. Computational tools and algorithms for designing customized synthetic genes. *Frontiers in Bioengineering and Biotechnology* vol. 2 (2014).
13. Li, L. M., Grassly, N. C. & Fraser, C. Genomic analysis of emerging pathogens: Methods, application and future trends. *Genome Biology* vol. 15 541 (2014).
14. Mahé, P. & Tournoud, M. Predicting bacterial resistance from whole-genome sequences using k-mers and stability selection. *BMC Bioinformatics* **19**, 383 (2018).
15. Francis, O. E. *et al.* Pathoscope: Species identification and strain attribution with unassembled sequencing data. *Genome Research* **23**, 1721–1729 (2013).
16. Hong, C. *et al.* PathoScope 2.0: A complete computational framework for strain identification in environmental or clinical sequencing samples. *Microbiome* **2**, 33 (2014).
17. Naccache, S. N. *et al.* A cloud-compatible bioinformatics pipeline for ultrarapid pathogen identification from next-generation sequencing of clinical samples. *Genome Research* **24**, 1180–1192 (2014).
18. Zaharia, M. *et al.* Faster and More Accurate Sequence Alignment with SNAP. (2011).
19. Zhao, Y., Tang, H. & Ye, Y. RAPSearch2: A fast and memory-efficient protein similarity search tool for next-generation sequencing data. *Bioinformatics* **28**, 125–126 (2012).
20. Byrd, A. L. *et al.* Clinical PathoScope: Rapid alignment and filtration for accurate pathogen identification in clinical samples using unassembled sequencing data. *BMC Bioinformatics* **15**, 262 (2014).
21. Miller, S. *et al.* Laboratory validation of a clinical metagenomic sequencing assay for pathogen detection in cerebrospinal fluid. *Genome Research* **29**, 831–842 (2019).
22. CosmosID/cosmosid-cli: Command line client and Python libraries for CosmosID API.
23. Yan, Q. *et al.* Evaluation of the cosmosid bioinformatics platform for prosthetic joint-associated sonicate fluid shotgun metagenomic data analysis. *Journal of Clinical Microbiology* **57**, (2019).

24. Albin, D. *et al.* SeqScreen: A biocuration platform for robust taxonomic and biological process characterization of nucleic acid sequences of interest. in *Proceedings - 2019 IEEE International Conference on Bioinformatics and Biomedicine, BIBM 2019* 1729–1736 (Institute of Electrical and Electronics Engineers Inc., 2019). doi:10.1109/BIBM47256.2019.8982987.
25. Qiao, W. *et al.* From mutations to mechanisms and dysfunction via computation and mining of protein energy landscapes 06 Biological Sciences 0601 Biochemistry and Cell Biology. *BMC Genomics* **19**, 671 (2018).
26. Goldstrohm, A. C., Hall, T. M. T. & McKenney, K. M. Post-transcriptional Regulatory Functions of Mammalian Pumilio Proteins. *Trends in Genetics* vol. 34 972–990 (2018).
27. Shiihashi, G. *et al.* Mislocated FUS is sufficient for gain-of-toxic-function amyotrophic lateral sclerosis phenotypes in mice. *Brain* **139**, 2380–2394 (2016).
28. Seneviratne, U. *et al.* S-nitrosation of proteins relevant to Alzheimer’s disease during early stages of neurodegeneration. *Proceedings of the National Academy of Sciences of the United States of America* **113**, 4152–4157 (2016).
29. Li, Y. H. *et al.* Clinical trials, progression-speed differentiating features and swiftness rule of the innovative targets of first-in-class drugs. *Briefings in Bioinformatics* **21**, 649–662 (2020).
30. Lai, A. C. & Crews, C. M. Induced protein degradation: An emerging drug discovery paradigm. *Nature Reviews Drug Discovery* vol. 16 101–114 (2017).
31. Zhou, N. *et al.* The CAFA challenge reports improved protein function prediction and new functional annotations for hundreds of genes through experimental screens. *Genome Biology* **20**, 244 (2019).
32. Törönen, P., Medlar, A. & Holm, L. PANNZER2: A rapid functional annotation web server. *Nucleic Acids Research* **46**, W84–W88 (2018).
33. Huerta-Cepas, J. *et al.* Fast genome-wide functional annotation through orthology assignment by eggNOG-mapper. *Molecular Biology and Evolution* **34**, 2115–2122 (2017).
34. Kulmanov, M. & Hoehndorf, R. DeepGOPlus: improved protein function prediction from sequence. *Bioinformatics* **36**, 422–429 (2019).
35. You, R. *et al.* NetGO: improving large-scale protein function prediction with massive network information. *Nucleic Acids Research* **47**, W379–W387 (2019).
36. Piovesan, D. & Tosatto, S. C. E. INGA 2.0: Improving protein function prediction for the dark proteome. *Nucleic Acids Research* **47**, W373–W378 (2019).
37. Shaikh, N. & Tarr, P. I. Escherichia coli O157:H7 Shiga toxin-encoding bacteriophages: Integrations, excisions, truncations, and evolutionary implications. *Journal of Bacteriology* **185**, 3596–3605 (2003).
38. Ondov, B. D. *et al.* Mash: Fast genome and metagenome distance estimation using MinHash. *Genome Biology* **17**, 132 (2016).
39. Titus Brown, C. & Irber, L. sourmash: a library for MinHash sketching of DNA. *The Journal of Open Source Software* **1**, 27 (2016).
40. Lu, J. & Salzberg, S. L. Ultrafast and accurate 16S rRNA microbial community analysis using Kraken 2. *Microbiome* **8**, 124 (2020).
41. Truong, D. T. *et al.* MetaPhlan2 for enhanced metagenomic taxonomic profiling. *Nature Methods* vol. 12 902–903 (2015).
42. Breitwieser, F. P., Baker, D. N. & Salzberg, S. L. KrakenUniq: Confident and fast metagenomics classification using unique k-mer counts. *Genome Biology* **19**, 198 (2018).
43. Menzel, P., Ng, K. L. & Krogh, A. Fast and sensitive taxonomic classification for metagenomics with Kaiju. *Nature Communications* **7**, 1–9 (2016).
44. Xiong, Y. *et al.* Transcriptomic characteristics of bronchoalveolar lavage fluid and peripheral blood mononuclear cells in COVID-19 patients. *Emerging Microbes and Infections* **9**, 761–770 (2020).
45. Franzosa, E. A. *et al.* Species-level functional profiling of metagenomes and metatranscriptomes. *Nature Methods* **15**, 962–968 (2018).
46. Jungo, F., Bougueleret, L., Xenarios, I. & Poux, S. The UniProtKB/Swiss-Prot Tox-Prot program: A central hub of integrated venom protein data. *Toxicon* **60**, 551–557 (2012).

47. Song, S. & Wood, T. K. Post-segregational Killing and Phage Inhibition Are Not Mediated by Cell Death Through Toxin/Antitoxin Systems. *Frontiers in Microbiology* **9**, (2018).
48. Bateman, A. UniProt: A worldwide hub of protein knowledge. *Nucleic Acids Research* **47**, D506–D515 (2019).
49. Liu, B., Zheng, D., Jin, Q., Chen, L. & Yang, J. VFDB 2019: A comparative pathogenomic platform with an interactive web interface. *Nucleic Acids Research* **47**, D687–D692 (2019).
50. Davis, J. J. *et al.* The PATRIC Bioinformatics Resource Center: Expanding data and analysis capabilities. *Nucleic Acids Research* **48**, D606–D612 (2020).
51. Urban, M. *et al.* PHI-base: The pathogen-host interactions database. *Nucleic Acids Research* **48**, D613–D620 (2020).
52. Gupta, A., Kapil, R., Dhakan, D. B. & Sharma, V. K. MP3: A Software Tool for the Prediction of Pathogenic Proteins in Genomic and Metagenomic Data. *PLoS ONE* **9**, e93907 (2014).
53. Coleman, B. *et al.* Diversified RACE Sampling on Data Streams Applied to Metagenomic Sequence Analysis. *bioRxiv* 852889 (2019) doi:10.1101/852889.
54. di Tommaso, P. *et al.* Nextflow enables reproducible computational workflows. *Nature Biotechnology* vol. 35 316–319 (2017).
55. Shah, N., Altschul, S. F. & Pop, M. Outlier detection in BLAST hits. *Algorithms for Molecular Biology* **13**, 7 (2018).
56. Langmead, B. & Salzberg, S. L. Fast gapped-read alignment with Bowtie 2. *Nature Methods* **9**, 357–359 (2012).
57. Eddy, S. R. Profile hidden Markov models. *Bioinformatics* vol. 14 755–763 (1998).
58. Finn, R. D. *et al.* Pfam: The protein families database. *Nucleic Acids Research* vol. 42 (2014).
59. Buchfink, B., Xie, C. & Huson, D. H. Fast and sensitive protein alignment using DIAMOND. *Nature Methods* vol. 12 59–60 (2014).
60. Kim, D., Song, L., Breitwieser, F. P. & Salzberg, S. L. Centrifuge: Rapid and sensitive classification of metagenomic sequences. *Genome Research* **26**, 1721–1729 (2016).
61. Suzek, B. E., Huang, H., McGarvey, P., Mazumder, R. & Wu, C. H. UniRef: comprehensive and non-redundant UniProt reference clusters. *Bioinformatics* **23**, 1282–1288 (2007).
62. Blom, J. *et al.* EDGAR 2.0: an enhanced software platform for comparative gene content analyses. *Nucleic acids research* **44**, W22–W28 (2016).
63. Prifti, E. *et al.* Interpretable and accurate prediction models for metagenomics data. *GigaScience* **9**, 1–11 (2020).
64. Carrieri, A. P. *et al.* Explainable AI reveals changes in skin microbiome composition linked to phenotypic differences. *bioRxiv* 2020.07.02.184713 (2020) doi:10.1101/2020.07.02.184713.
65. Kingma, D. P. & Ba, J. L. Adam: A method for stochastic optimization. in *3rd International Conference on Learning Representations, ICLR 2015 - Conference Track Proceedings* (International Conference on Learning Representations, ICLR, 2015).
66. Pedregosa FABIANPEDREGOSA, F. *et al.* *Scikit-learn: Machine Learning in Python Gaël Varoquaux Bertrand Thirion Vincent Dubourg Alexandre Passos PEDREGOSA, VAROQUAUX, GRAMFORT ET AL. Matthieu Perrot. Journal of Machine Learning Research* vol. 12 (2011).
67. Chollet, F. & others. Keras. (2015).
68. Bolger, A. M., Lohse, M. & Usadel, B. Trimmomatic: a flexible trimmer for Illumina sequence data. *Bioinformatics* **30**, 2114–2120 (2014).

Acknowledgements

Our appreciation goes out to Chris Hulme-Lowe, Danielle LeSassier, Nicolette Albright, Katharina Weber, Veena Palsikar, Oana Lungu, Curt Hewitt, Pravin Muthu, Cynthia DiPaula, Isaac Mayes, Don Bowman, Christopher Grahlmann, and Leslie

Parke for their efforts in assisting with the development of the UniProt queries, internal organization of the curation data, and assistance in software development and testing at Signature Science, LLC. We would also like to acknowledge project team contributions of Jason Hauzel, Kristófer Thorláksson, Manoj Deshpande, Brendan Joyce, Garrit Nickel, Steffen Matheis, Larissa Wagnerberger, Vijayadhaarani Vijayaarunachalam, Mikael Lindvall, and Adam Porter at Fraunhofer CMA USA for their support in software quality assurance and development of the HTML report generator, Jeremy Selengut of the University of Maryland for sharing his insights into viral pathogenesis, Jim Gibson of Signature Science, LLC for graphics development, and Letao Qi, Jacob Lu, and Chris Jermaine of Rice University for insightful discussions and work specific to the machine learning algorithms. Thanks to Jody Proescher, Ron Jacak, Kristina Zudock and Briana Vecchio-Pagan from Johns Hopkins University Applied Physics Lab for their helpful discussions about pathogenesis ontologies and assistance with deployment and testing of our software on their servers. SeqScreen software development has significantly benefited from the feedback of Elizabeth Vitalis and Ian Fiddes at Inscripta and Cory Bernhards' team at U.S. Army Combat Capabilities Development Command Chemical Biological Center. We are thankful for all the time and effort provided by end users to test early versions of our software, recommend improvements, and guide its application to current challenges in pathogen detection, synthetic biology, and genome engineering. Finally, we would like to thank IARPA and all of our SeqScreen end users for their helpful feedback and support over the course of the Fun GCAT program to bring this software to where it is today.

All of the co-authors were either fully or partially supported by the Fun GCAT program from the Office of the Director of National Intelligence (ODNI), Intelligence Advanced Research Projects Activity (IARPA), via the Army Research Office (ARO) under Federal Award No. W911NF-17-2-0089. The views and conclusions contained herein are those of the authors and should not be interpreted as necessarily representing the official policies or endorsements, either expressed or implied, of the ODNI, IARPA, ARO, or the US Government.

Author Contributions

K.T. and T.T. designed the SeqScreen concept. A.B., B.K., D.A, T.T., M.D., L.E., Z.Q., and D.N. developed the software. G.G, A.K., and K.T. designed and implemented the biocuration framework. A.B., B.K. T.T. and S.S. designed and implemented the machine learning framework. N.S. and M.P. designed outlier detection. A.B., B.K., Z.Q., E.R produced results for benchmarking. A.B., L.E., G.G., S.S., N.S., M.P, K.T., and T.T. contributed to writing the manuscript. All authors read and approved the manuscript.

FIGURES

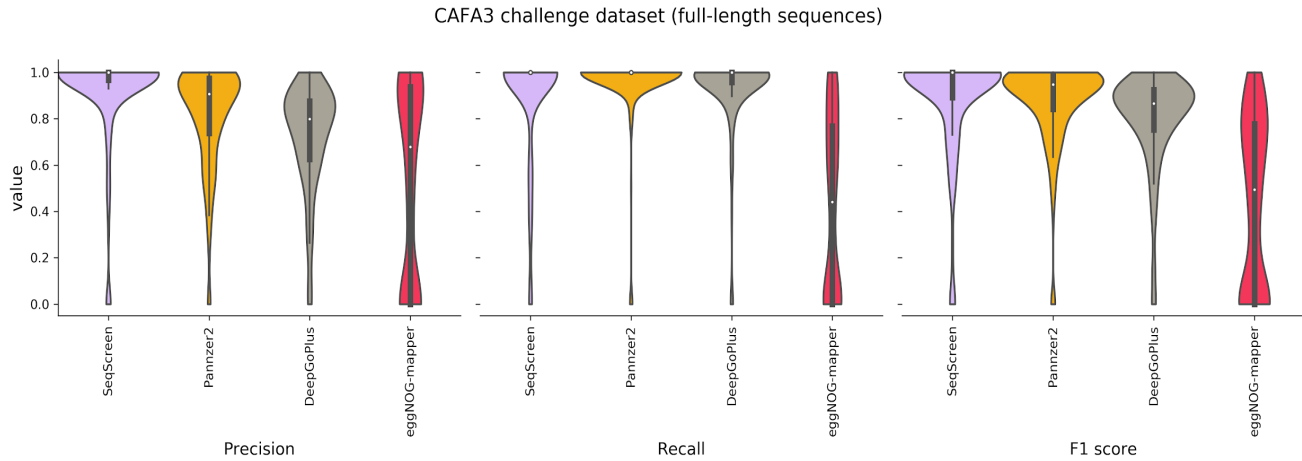


Fig. 1. Functional annotation results on full-length proteins. SeqScreen shows the highest precision of all tools followed by PANNZER2 and DeepGOPlus. eggNOG-mapper's precision is the lowest among all tools. In terms of recall, PANNZER2 followed by DeepGOPlus has the highest performance. They are followed by SeqScreen and eggNOG-mapper. SeqScreen still reported the highest F1 score among all tools.

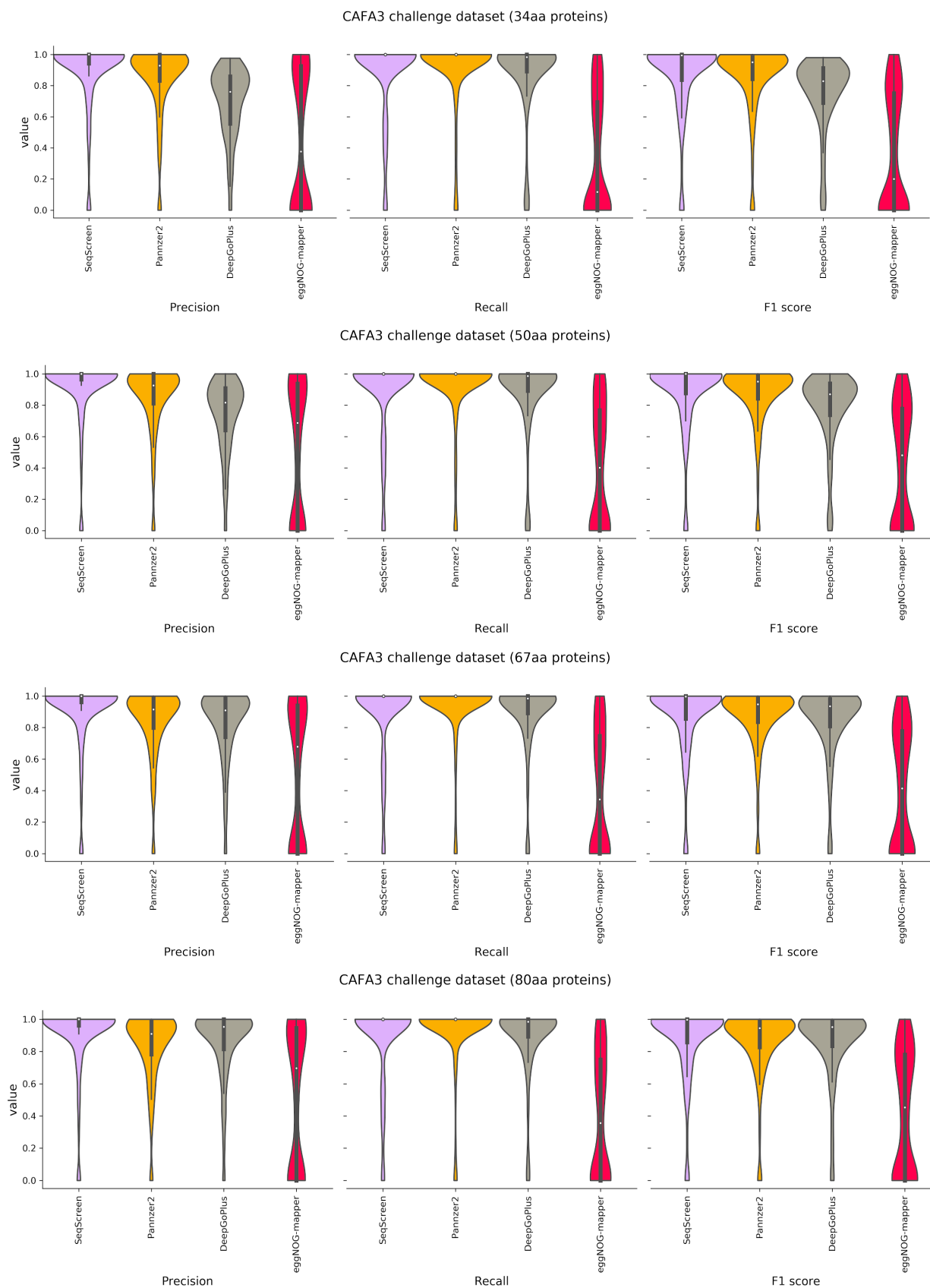


Fig. 2. Functional annotation results on 250 proteins obtained from CAFA-3 training datasets for 34, 50, 67 and 80 amino acids (aa). The first figure on each panel represents precision followed by recall and F1 score. We observe that SeqScreen consistently achieves the best performance for both precision and recall and by extension the best F1 score for all the sub-lengths. The order of the tools is in decreasing order of their median F1 score. PANNZER2 maintains the highest recall through all the lengths while its precision increases slightly from 34aa to 67aa. eggNOG-mapper increases its precision, recall and F1 score from 34aa to 67aa but only sees marginal improvement thereafter. DeepGOPlus improves its precision above that of PANNZER2 at 80aa.

Top Performing models: Positive Label Precision and Recall per FunSoC

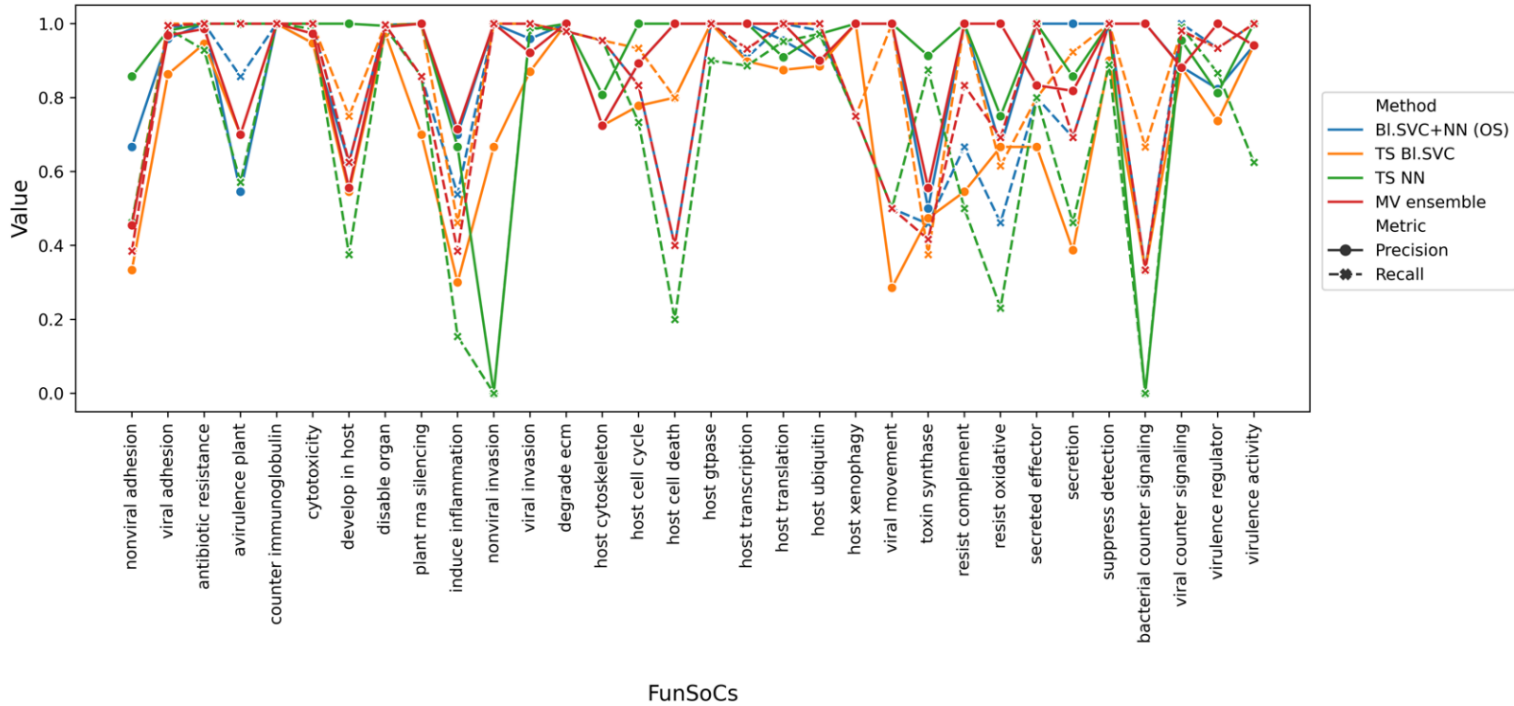
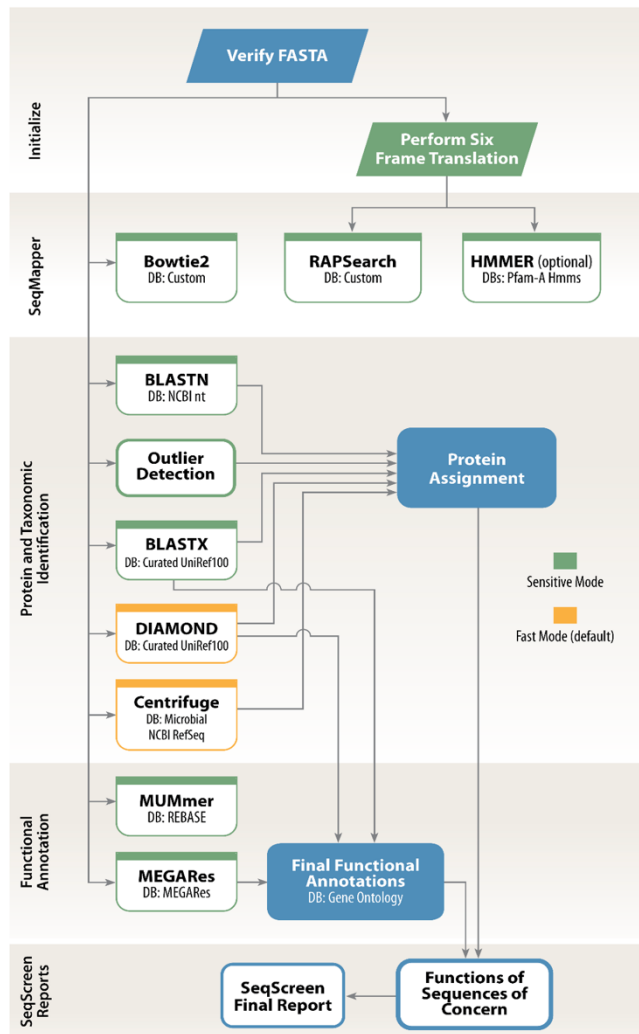


Fig. 3. Positive label precision and recall per FunSoC for the four ML models BI. SVC+NN (OS) (in blue), TS NN (in green), TS Bl. SVC (in orange), and MV ensemble (in red). Precision is in solid lines and Recall is in dotted lines. TS Bl. SVC shows the best overall recall, whereas TS NN consistently has the highest precision across most of the 32 FunSoCs. In hard-to-classify FunSoCs like *nonviral invasion* and *bacterial counter signaling* TS NN performs poorly indicating a model with a high degree of variance. Similarly, TS Bl. SVC suffers from poor precision in most cases. The Majority Vote Classifier improves on the BI. SVC+NN (OS) and finds an optimal balance between precision and recall across all FunSoCs.

		FunSoCs									
Isolate genome (SRA accession)		disable organ	cytotoxicity	degrade ecm	induce inflammation	secreted effector	secretion	antibiotic resistance	bacterial counter signaling	counter immunoglobulin	virulence regulator
Bacteria	(a) <i>E.coli</i> K12 MG1655 (DRR198806)		<i>hlyE</i>			<i>tir</i>	17 genes identified*	35 genes identified*			
	(b) <i>E.coli</i> O157:H7 (DRR198804)		<i>stxB, hlyE</i>			<i>espF(U), tir</i>	15 genes identified*	34 genes identified*			<i>espF(U), nleF</i>
	(c) <i>C.sporogenes</i> (SRR8758382)						T3SA	<i>bla, uppP, pbbA</i>	<i>moaC</i>		
	(d) <i>C.botulinum</i> (SRR8981313)	<i>botA</i>	<i>orf-X2</i>	<i>botA</i>				<i>bla, uppP, pbbA</i>	<i>moaC</i>		<i>botA</i>
	(e) <i>S.dysgalactiae</i> (SRR12825903)		<i>SLO</i>				<i>comYC</i>	<i>uppP, pilA</i>		<i>spg</i>	
	(f) <i>S.pyogenes</i> (ERR1735064)		<i>SLO</i>		<i>speB, speH</i>		<i>comYC</i>	<i>uppP</i>			
	(g) <i>S.salivarius</i> (SRR11910125)						<i>cglC, comGC</i>	<i>mprF, uppP, pbbA</i>			
	(h) <i>L.gasseri</i> (SRR11910134)							<i>mprF, aac(3)</i>			

Fig. 4. Pathogen identification of hard-to-classify pathogens: FunSoCs Assigned to Genes by SeqScreen. Abbreviated gene names are listed in pink cells if at least one read from the gene had an UniProt e-value < 0.0001, was assigned a FunSoC, and was from the expected genus (i.e., Escherichia or Shigella, Clostridium, Streptococcus, Lactobacillus). FunSoCs with at least one gene that met the criteria for detection in at least one isolate were included in the table. The removal of genes from genera that were not expected in these bacterial isolates allowed for removal of genes that were likely derived from likely contaminating organisms (e.g., PhiX Illumina sequencing control). An expanded table for cells denoted by (*) and complete gene names are listed within each cell in Supplementary Table S3. (a and b) *E. coli* O157:H7 is shown to have presence of the *shiga toxin (stxB)* as seen in the *cytotoxicity* FunSoC, as well as an additional hit to the *secreted effector protein (espF(U))*, labelled with *secreted effector* and *virulence regulator* FunSoCs, compared to *E.coli* K12 MG1655. (c and d) *C. botulinum* showed four distinct FunSoCs (*disable organ*, *cytotoxicity*, *degrade ecm* and *virulence regulator*) and presence of the *botA* and *orf-X2* genes compared to *C. sporogenes*. (e and f) *S. pyogenes* showed presence of the *induce inflammation* FunSoC in contrast to the near neighbor pathogen *S. dysgalactiae* with the *counter immunoglobulin* FunSoC. (g and h). *S. salivarius* and *L. gasseri* are well-known commensals that are generally considered harmless. Both show presence of antibiotic resistance genes, while *S. salivarius* also contains some genes associated with *secretion*. The commensals have hits to the least number of FunSoCs.

A. SeqScreen Workflows



B. SeqScreen Biocuration-Machine Learning Framework

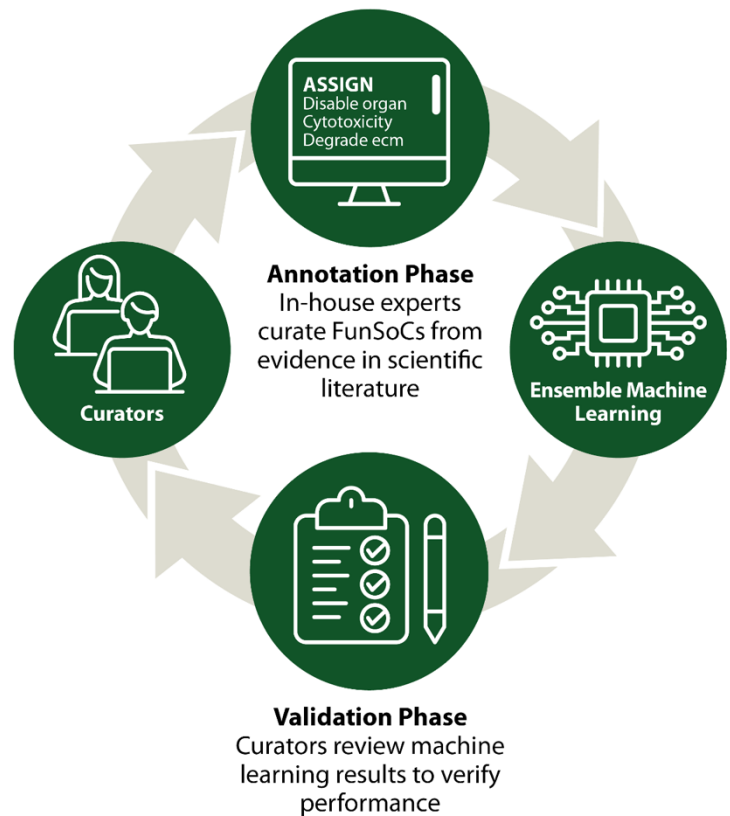


Fig. 5. SeqScreen overview. (A.) SeqScreen Workflow: This figure outlines the various modules and workflows of the SeqScreen pipeline. Boxes in green indicate that these modules are only run in the sensitive mode. The boxes in yellow are run in the fast mode, while the ones in blue are common to both modes. In addition to the two different modes, SeqScreen also contains optional modules that can be run based on the parameters provided by the user. (B.) SeqScreen Human-in-the-loop Framework: Includes initial annotation and curation of training data by manual curation. The data is used to train Ensemble ML models. The results obtained and selected feature weights are passed on back to biocurators to fine tune features and uniprot queries which form a new set of refined training data for the Ensemble model.

SeqScreen v1.3.1

Input files last modified:

88/2020 16:16:52
Sequence file 07/21/20 09:07:05
Elast output 88/2020 16:15:27

Summary:

Sequences provided 10

Per-sequence overview

[Filter](#)

1

Query	Length	Organism	Gene Name	GO Terms	Adherence HostCell Nonviral	Adherence HostCell Viral	Antibiotic Resistance	Avirulence	Bind Host Cytoline	Bind Host Immunoglobulin	Cytotoxicity	Development In Host	Disable Organ System	Host RNA Silencing Viral	Induce Inflammation	Invasion Host Cell Nonviral	Invasion Host Cell Viral
Bacillus_anthraxis_str_Ames	500	Bacillus cereus AH820	DNA replication and repair protein RecF	<ul style="list-style-type: none"> 1. DNA replication 2. SOS response 3. single-stranded DNA binding Show more	0	0	0	0	0	0	0	0	0	0	0	0	0
Thermus_aquaticus_Y51MC23	500	Thermus aquaticus Y51MC23	Enolase	<ul style="list-style-type: none"> 1. phosphopyruvate hydratase activity 2. lyase activity 3. glycolytic process Show more	0	0	0	0	0	0	0	0	0	0	0	0	0
Zaire_ebolavirus	500	Zaire ebolavirus	Envelope glycoprotein	<ul style="list-style-type: none"> 1. suppression by virus of host innate immune response 2. evasion or tolerance by virus of host immune response 3. protein binding Show more	0	1	0	0	0	0	0	0	0	0	0	0	1

Fig. 6.: HTML report output from SeqScreen. This is a screenshot of the interactive HTML page that outputs each query sequence in the file, the length, the gene name (if found), and GO terms associated with it. It also outputs the presence (or absence) of each of the 32 FunSoCs by denoting a 1 (or 0) in the given field.

TABLES

Table 1: Comparison of SeqScreen to related tools. State-of-the art functional annotation tools and taxonomy-based pathogen identification tools are listed in this table, with checkmarks for features present.

Tool	Tool Category	Default DB	Curated and Custom DBs	Runs on Illumina reads	Functional Characterization (gene based)	Functional Characterization (gene fragments)	Pathogen Sequence Identification (taxonomy based)	Pathogen Sequence Identification (function based)
PANNZER2	Functional Characterization	UniProtKB			✓	✓		
DeepGOPlus	Functional Characterization	UniProt			✓	✓		
eggNOG-mapper	Functional Characterization	CoG, eggNoG Protein DB			✓	✓		
HUMAnN2	Functional Characterization	UniRef, MetaCyc and MiniPath			✓	✓		
Mash dist	Taxonomy based Pathogen ID	RefSeq NCBI nt DB	✓	✓			✓	
Sourmash	Taxonomy based Pathogen ID	RefSeq NCBI nt DB and GenBank	✓	✓			✓	
PathoScope	Taxonomy based Pathogen ID	RefSeq NCBI nt DB	✓	✓			✓	
KrakenUniq	Taxonomy based Pathogen ID	RefSeq NCBI nt DB	✓	✓			✓	
Kraken2	Taxonomy based Pathogen ID	RefSeq NCBI nt DB	✓	✓			✓	
MetaPhlan2	Taxonomy based Pathogen ID	Integrated Microbial Genomes (IMG) system	✓	✓			✓	
Kaiju	Taxonomy based Pathogen ID	NCBI nr	✓	✓			✓	
SeqScreen (this paper)	Taxonomic Classification + Functional Characterization + Function based Pathogen ID	UniProt/GenBank/RefSeq	✓	✓	✓	✓	✓	✓

Table 2. The Accuracy, Exact Match Ratio, Micro and Macro F1 Score, Macro Recall and Precision of the different ML models. The models we considered were Balanced SVC (Feature Selection) + Neural Network Classification using Oversampling (Bl. SVC+NN (OS)), Two Stage Detection + Classification Neural Networks (TS NN), Two Stage Detection + Classification Balanced Support Vector Classifier (TS Bl. SVC), and the Majority Vote Ensemble Classifier (MV ensemble). TS NN had the highest positive label (PL) precision and TS Bl.SVC had the highest positive label (PL) Recall, while Bl. SVC+NN (OS) had the best balance between precision and recall. Majority Vote Ensemble improved on the results of the three classifiers as conveyed by both the high precision and recall the method achieves.

Model	Accuracy	Exact Match Ratio	Micro F1 Score	Macro F1 Score	Macro Recall	Macro Precision	Mean PL Precision	Mean PL Recall
Bl. SVC+NN (OS)	0.9997	0.9924	0.9859	0.8210	0.8039	0.8716	0.8759	0.8180
TS NN	0.9997	0.9924	0.9359	0.6934	0.6445	0.8011	0.8893	0.6988
TS Bl.SVC	0.9996	0.9893	0.8692	0.7047	0.8310	0.6492	0.7382	0.8869
MV ensemble	0.9997	0.9934	0.9424	0.7998	0.8016	0.8453	0.9003	0.8273

Table 3. Pathogen and near neighbor classification. SRA represents the SRA id of the sample, **True Organism** represents the actual bacterial strain or species, and the remaining columns indicate the results for the indicated method using the parameters detailed in the Methods section. Green cells indicate that the tool assigned a correct strain-level call, yellow indicates a correct species-level call, and red indicates an incorrect species-level call. The following tools and databases were run: Mash dist (RefSeq 10k), Sourmash (RefSeq + GenBank), PathoScope (PathoScope DB), Kraken 2 (Mini and full Kraken2 DB produced the same results), KrakenUniq (MiniKraken 8GB), MetaPhlAn2 (default) and Kaiju (index of NCBI nr + euk). Even with a complete database, *C. sporogenes* was wrongly classified as *C. botulinum* by PathoScope, Kraken2, and KrakenUniq. Mash dist, Sourmash, MetaPhlAn2, and Kaiju predicted *C. sporogenes* correctly. *C. botulinum* was incorrectly classified as *C. sporogenes* by Mash dist, Sourmash, and MetaPhlAn2. *S. dysgalactiae* was predicted as *S.pyogenes* by PathoScope. All tools correctly called *S. pyogenes*. The *E. coli* strains were challenging for most tools. The pathogenic *E. coli* O157:H7 was correctly called by Mash dist, Sourmash, PathoScope, Kraken2 and KrakenUniq. MetaPhlAn and Kaiju could only make a species level assignment. In contrast, the commensal *E. coli* K12 MG1655 was the most challenging as only Mash dist and Sourmash got the strain level assignment correct. MetaPhlAn2 and Kaiju could make only species level assignments, and PathoScope, Kraken2, and KrakenUniq called it as strains *E. coli* BW2952, *E. coli* O157:H7, and *E. coli* O145:H28, respectively.

SRA	True Organism	Mash dist	Sourmash	PathoScope	Kraken2	KrakenUniq	MetaPhlAn2	Kaiju
DRR198806	<i>E. coli</i> K12 MG1655	Equivalent hits for <i>E. coli</i> K12 and SQ37	<i>E. coli</i> K12	<i>E. coli</i> BW2952	<i>E. coli</i> O157:H7	<i>E. coli</i> O145:H28	<i>E. coli</i>	<i>E. coli</i>
DRR198804	<i>E. coli</i> O157:H7	<i>E. coli</i> O157:H7	<i>E. coli</i> O157:H7	<i>E. coli</i> O157:H7	<i>E. coli</i> O157:H7	<i>E. coli</i> O157:H7	<i>E. coli</i>	<i>E. coli</i>
SRR8758382	<i>C. sporogenes</i>	<i>C. sporogenes</i>	<i>C. sporogenes</i>	<i>C. botulinum</i>	<i>C. botulinum</i>	<i>C. botulinum</i>	<i>C. sporogenes</i>	<i>C. sporogenes</i>
SRR8981313	<i>C. botulinum</i>	<i>C. sporogenes</i>	<i>C. sporogenes</i>	<i>C. botulinum</i>	<i>C. botulinum</i>	<i>C. botulinum</i>	<i>C. sporogenes</i>	<i>C. botulinum</i>
SRR12825903	<i>S. dysgalactiae</i>	<i>S. dysgalactiae</i>	<i>S. dysgalactiae</i>	<i>S. pyogenes</i>	<i>S. dysgalactiae</i>	<i>S. dysgalactiae</i>	<i>S. dysgalactiae</i>	<i>S. dysgalactiae</i>
ERR1735064	<i>S. pyogenes</i>	<i>S. pyogenes</i>	<i>S.pyogenes</i>	<i>S. pyogenes</i>	<i>S. pyogenes</i>	<i>S. pyogenes</i>	<i>S. pyogenes</i>	<i>S. pyogenes</i>

Table 4. Simulating a novel pathogen. Mash dist and PathoScope were run on pathogen sequences and their near neighbors with the corresponding truth species removed in their respective databases to simulate an example of classifying a novel pathogen not in the database. **SRA** represents the SRA id of the sample, **True Organism** represents the actual bacterial strain or species, **Mash dist** represents the Mash results on each of the samples (with the truth organism species or strain removed from its sketch database), and Pathoscope represents the PathoScope results on each of the samples (with the truth organism species or strain removed from its database). In three of the cases, *C. sporogenes*, *C. botulinum* and *S. pyogenes*, Mash dist classified the organism as its near neighbor - *C. botulinum*, *C. sporogenes* and *S. dysgalactiae*, respectively. *S. dysgalactiae* was classified as *S. sp. NCTC 11567* whereas the commensal *E. coli K12* and pathogenic *E. coli O157:H7* were classified as *E. coli O16:H48* and *E. coli 2009C-3554*, respectively. PathoScope only classified two pathogens, *C. sporogenes* and *C. botulinum*, as their nearest neighbor counterparts. *S. dysgalactiae* was classified as *S. intermedius*, whereas *S. pyogenes* was classified as *S. infantarius*. *E. coli K12* was only classified at the species level, while the pathogenic strain *E. coli O157:H7* was classified as *E. coli xuzhou21*.

SRA	True Organism	Mash dist	PathoScope
DRR198806	<i>E. coli K12 MG1655</i>	<i>E. coli O16:H48</i>	<i>E. coli</i>
DRR198804	<i>E. coli O157:H7</i>	<i>E. coli 2009C-3554</i>	<i>E. coli Xuzhou21</i>
SRR8758382	<i>C. sporogenes</i>	<i>C. botulinum</i>	<i>C. botulinum</i>
SRR8981313	<i>C. botulinum</i>	<i>C. sporogenes</i>	<i>C. sporogenes</i>
SRR12825903	<i>S. dysgalactiae</i>	<i>S. sp. NCTC 11567</i>	<i>S. intermedius</i>
ERR1735064	<i>S. pyogenes</i>	<i>S. dysgalactiae</i>	<i>S. infantarius</i>